Analytica Chimica Acta 1221 (2022) 340128

Contents lists available at ScienceDirect

Analytica Chimica Acta

journal homepage: www.elsevier.com/locate/aca

Real matrix-matched standards for quantitative bioimaging of cytosolic proteins in individual cells using metal nanoclusters as immunoprobes-label: A case study using laser ablation ICP-MS detection

Ana Lores-Padín [a], Beatriz Fernández [a,b,*], Montserrat García [b,c], Héctor González-Iglesias [b,d], Rosario Pereiro [a,b,**]

[a] Department of Physical and Analytical Chemistry, University of Oviedo, Julian Claveria 8, 33006, Oviedo, Spain
[b] Instituto Universitario Fernández-Vega, Fundación de Investigación Oftalmológica, Universidad de Oviedo, Oviedo, Spain
[c] Instituto Oftalmológico Fernández-Vega, Avda. Dres. Fernández-Vega, 34, 33012, Oviedo, Spain
[d] Department of Technology and Biotechnology of Dairy Products, Instituto de Productos Lácteos de Asturias, Consejo Superior de Investigaciones Científicas (IPLA-CSIC), Villaviciosa, Spain

HIGHLIGHTS

- Quantitative imaging of proteins in individual cells was performed by LA-ICP-MS.
- The matrix-matched calibration standards fully mimic the cultured cells matrix.
- Single-cell laboratory standards based on cells supplemented with AuNCs were used.
- HRPEsv@AuNCs cells standards were characterised by ICP-MS and LA-ICP-MS.
- Au nanoclusters were used as specific antibody labels to develop AuNCs-immunoprobes.

GRAPHICAL ABSTRACT

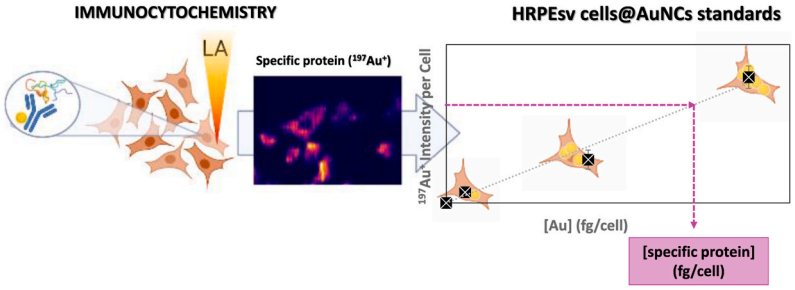

ARTICLE INFO

Keywords:
Laser ablation ICP-MS
Matrix-matched calibration
Quantitative imaging of proteins
Metal nanoclusters
Cytosolic proteins

ABSTRACT

The persistent lack of adequate matrix-matched reference materials still hinders the quantitative analysis of elements and biomolecules in biological samples by LA-ICP-MS. This fact is especially critical in cell cultures due to their complex matrix. In this work, we propose a novel matrix-matched calibration strategy, which fully mimics the matrix of cultured cells, by using the same cell line of the sample to create laboratory standards. As a model case, the quantitative imaging of two cytosolic proteins (MT2A and APOE) in individual HRPEsv cells was performed by LA-ICP-MS, both in cells subjected to inflammation with cytokine Interleukin-1α (IL-1α) and controls (CT). A single biomarker strategy using Au nanoclusters (AuNCs) as specific antibody labels was employed for the analysis of the selected proteins in individual cells by LA-ICP-MS. HRPEsv cells supplemented with suspensions containing nude AuNCs was employed to generate single-cell laboratory standards (HRPEsv cells@AuNCs). The preparation and characterization of the single-cell laboratory standards by both ICP-MS and LA-ICP-MS were optimized as well as the data treatment protocol required for obtaining the quantitative

* Corresponding author. Department of Physical and Analytical Chemistry, University of Oviedo, Julian Claveria 8, 33006, Oviedo, Spain.
** Corresponding author. Department of Physical and Analytical Chemistry, University of Oviedo, Julian Claveria 8, 33006, Oviedo, Spain.
E-mail addresses: fernandezbeatriz@uniovi.es (B. Fernández), mrpereiro@uniovi.es (R. Pereiro).

https://doi.org/10.1016/j.aca.2022.340128
Received 15 March 2022; Received in revised form 19 May 2022; Accepted 24 June 2022
Available online 27 June 2022

distribution of the proteins in individual cells. The mass of APOE and MT2A per cell in CT and IL1α−treated HRPEsv cells analysed by LA-ICP-MS using the proposed matrix-matched calibration were successfully corroborated with commercial ELISA kits. In addition, quantitative real time polymerase chain reaction (qPCR) analyses were performed to study the proteins gene expression.

1. Introduction

Inductively coupled plasma-mass spectrometry (ICP-MS) has been widely used for the determination of trace elements as well as metal-based tags in biological fluids [1]. In general, such biological fluids are submitted to a certain treatment prior to ICP-MS analysis and a homogeneous solution is traditionally analysed by conventional nebulization ICP-MS. However, there are certain type of samples where the determination of bulk information is not enough, such as cultured cells. It is well known that cells of the same origin, even under the same physiological conditions or external stimuli, can respond differently, generating cell-to-cell variations [2]. Therefore, there is a need to develop new analytical methodologies that allow not only the identification but also the quantification of target elements and biomolecules at the single cellular level.

Concerning ICP-MS detection, new technological advances, such as single cell (sc) introduction by nebulization, allows cell-to-cell measurements [3]. Nevertheless, subcellular distribution cannot be obtained by sc-ICP-MS and, in addition, risks of non-representative sampling due to size-dependent cellular losses in the transport towards the ICP-MS can take place. Both aspects could be overcome by direct solid sampling with laser ablation (LA) combined to ICP-MS detection [4]. LA-ICP-MS offers interesting capabilities for elemental and isotopic analysis, including high spatial resolution (in the low μm range) and sensitivity (μg g^{-1} to ng g^{-1}). Concerning imaging studies, LA-ICP-MS has shown a huge potential for elemental imaging in biological tissues [5]. Additionally, in combination with an immunoassay protocol using elemental-labelled antibodies the imaging of specific proteins can also be achieved [6]. Most of the articles tackled with the imaging of proteins by LA-ICP-MS have been focused onto the proteins distribution along tissue sections. Nevertheless, with the incursion of new technologies (i.e., ultra-fast ablation cells, the use of small laser spot size diameters and new LA-ICP interfaces that enhance the transport of the laser-generated aerosol as well as the sensitivity) studies related to cell cultures have been also addressed by LA-ICP-MS.

Most recently published LA-ICP-MS cellular studies are focused on the distribution of naturally present [7] or supplemented elements [8] as well as the uptake and metabolism of metal-based nanoparticles (MNPs) [9,10]. Additionally, target biomolecules can be detected through metal-labelling strategies. Single lanthanide complexes such as DOTA, polymeric tags containing several lanthanides (i.e., MAXPAR®) and MNPs have been reported for such purpose [6,11]. Noteworthy is the use of LA coupled to CyTOF MS which allows to obtain the simultaneous distribution of dozens of biomolecules by multi-metal-label detection imaging [12].

Nevertheless, the persistent lack of adequate matrix-matched materials still hinders the quantitative analysis of biomolecules in cells by LA-ICP-MS. Several works have recently reported the determination of metals and biomolecules in cells using customized calibration approaches. Drescher et al. [10] proposed the use of nitrocellulose membranes spiked with NPs suspensions for the determination of AuNPs and AgNPs in eukaryotic cells. This strategy was improved by Arakawa et al. [13,14] using micro-array spotter to reduce the size of the dried droplets of NPs suspension for the quantitative AgNPs distribution in 3D spheroids. Also, Wang et al. [15] used dried residues of picodroplets ejected by a commercial inkjet printer for the quantification of internalized AuNPs. Additionally, microarray metal spiked gelatines as standards for Cu quantification [16] or for the determination of membranous receptor (specific labelled with La-chelate) in breast cancer cells was reported by Vanhaecke's group [17]. There are also some works focused on the specific cell membrane biomolecule quantification using peptide-Au clusters as tags and dried metal spiked droplets residues as standards [18–20]. In any case, although the proposed calibration strategies tent to mimic the matrix of individual cells, they do not completely fulfil the characteristics of their complex nature.

In the current work, we propose a novel matrix-matched calibration strategy which fully mimics the complex matrix of cultured cells to perform the quantitative imaging of proteins in individual cells by LA-ICP-MS. As a proof of concept, the sequential determination of two cytosolic proteins (metallothionein 2A and apolipoprotein E; MT2A and APOE) in individual human retinal pigment epithelial immortalized cells (HRPEsv) was pursued by LA-ICP-MS, both in cultured cells subjected to inflammation with the cytokine Interleukin-1α (IL1α) and controls (CT). Fluorescent Au nanoclusters (AuNCs) were used as specific antibody labels to develop AuNCs-immunoprobes. Aiming to ensure full matrix-matched calibration, HRPEsv cells supplemented with suspensions containing nude AuNCs were prepared to generate single-cell laboratory standards (HRPEsv@AuNCs cells). To corroborate the quantitative results obtained for APOE and MT2A by LA-ICP-MS in HRPEsv cells, commercial ELISA kits were employed, and quantitative real time polymerase chain reaction (qPCR) analyses were performed to study their gene expression.

2. Experimental

Details related to the reagents employed for the synthesis and characterization of the AuNCs-immunoprobes, the culture and incubation of HRPEsv cells, the immunocytochemistry (ICC) assays with Alexa® fluorophores, as well as the qPCR and ELISA analyses are collected at **Supplementary Material.** Furthermore, protocols for the synthesis and characterization of AuNCs and AuNCs-immunoprobes are also described at **Supplementary Material**. Fig. 1 shows a workflow of the experimental implemented for the quantitative analysis of APOE and MT2A in HRPEsv cells by LA-ICP-MS.

2.1. Experimental methods

2.1.1. HRPEsv cell culture and pro-inflammatory treatment

HRPEsv cells were seeded onto different supports (e.g., flasks, 6-well-plate or chamber slides) at different concentrations ($6{\cdot}10^4$–$20{\cdot}10^6$ cells/well) depending on the assay, i.e., ELISA, qPCR, fluorescence, liquid nebulization ICP-MS or LA-ICP-MS. The HRPEsv immortalized cells were cultured at 37 °C in a 5% CO_2 incubator using Dulbecco's modified eagle medium/nutrient mixture F-12 (DMEMF12, Invitrogen) supplemented with 10% (v/v) fetal bovine serum (FBS) and 1% (v/v) penicillin/streptomycin (P/S). Once cells were confluent in each selected support, the medium was changed to CD hybridoma free medium (Gibco) supplemented with 5% L-glutamine and 1% P/S after washing with PBS once. 24 h later, cultured HRPEsv cells were either non-treated (i.e., control cells) or treated with 100 ng mL^{-1} of IL1α (Gold Bio) for 48 h. Subsequently, in order to carry out the ICC assay with the AuNCs-immunoprobes for the target protein analysis by fluorescence or LA-ICP-MS, seeded cells were washed with PBS and fixed, adding 400 μL of 4% paraformaldehyde per well for 10 min at room temperature (RT). Later, after washing with PBS once, the fixed cells were stored in the refrigerator in PBS to prevent possible drying and cell breakage. Specific details regarding HRPEsv cells preparation for ELISA assays and qPCR analyses (in this last case to study APOE and MT2A gene expression) are

collected at **Supplementary Material**.

2.1.2. Immunocytochemical assays for APOE and MT2A determination in HRPEsv cells using AuNCs-immunoprobes

ICC assays for the determination of the two selected cytosolic proteins in HRPEsv cells were carried out using a single biomarker strategy by means of sequentially use two AuNCs-immunoprobes (AuNCs:anti-h-APOE and AuNCs:anti-h-MT2A) on both CT and IL1α-treated cells. Detection of the AuNCs-immunoprobes fluorescence was carried out for the localization of APOE and MT2A in HRPEsv cells, whereas an indirect detection (due to fluorophore Alexa® emission) was used to determine the optimum concentration of the primary antibodies employed in the ICC assay.

The ICC protocol steps followed with HRPEsv cells for MS or fluorescence detection include: (i) Permeabilisation of the cell membranes: 400 μL of PBS with 0.1% triton X-100 for 30 min; (ii) Washing (3 times): 400 μL of PBS-0.05% tween-20; (iii) Blocking: 400 μL PBS with 10% donkey serum and 1% BSA for 1 h of incubation; (iv) Overnight incubation at 4 °C of the AuNCs-immunoprobes (400 μL of 10 μg mL^{-1} AuNCs:anti-h-APOE or 400 μL of 5 μg mL^{-1} AuNCs:anti-h-MT2A, referring to the antibody concentration) in PBS with 5% donkey serum and 1% BSA; and (v) Washing with 400 μL PBS (3 times). In the case of HRPEsv cells analysed by LA-ICP-MS, they were kept in PBS in the chamber slides until the analysis to ensure preservation of cells integrity (PBS was removed just before LA-ICP-MS analysis). The additional steps for fluorescence detection include: (vi) Incubation with secondary antibody (only for indirect detection) Alexa®594:goat antirabbit IgG and Alexa® 488:donkey antigoat IgG for respectively detecting anti-h-MT2A and anti-h-APOE, for 2 h at RT and in the darkness; (vii) Washing 3 times with PBS; (viii) Nuclei were counterstained by addition of 4',6-diamino phenylindole (DAPI, Thermo Fisher Scientific) stain for 10 min (RT and darkness); (ix) Washing step with PBS; and (x) Addition of a drop of fluorescence mounting medium (Dako, Agilent, USA) and placement of a coverslip over it.

Negative controls (for CT and IL1α−treated samples) were analysed by fluorescence microscopy and LA-ICP-MS. Negative immunoassay controls (i.e., without the primary antibody) were prepared for indirect fluorescence analysis to ensure specificity of the secondary antibody. In the case of direct fluorescence (AuNCs-immunoprobes) and LA-ICP-MS measurements, negative controls using AuNCs without the primary antibody were prepared to ensure that nonspecific interactions of AuNCs within the cell are not observed.

2.1.3. Preparation of "single-cell laboratory standards": HRPEsv cells@AuNCs

In order to determine the proteins concentration in HRPEsv cells by LA-ICP-MS, HRPEsv cells were also employed to prepare matrix-matched calibration standards. As detailed in the workflow of Fig. 1, HRPEsv cells supplemented with suspensions containing nude AuNCs (HRPEsv cells@AuNCs) were employed as single-cell laboratory standards. For such purpose, HRPEsv cultured cells were prepared in parallel and characterised either by conventional nebulization ICP-MS after mineralization of the cells (average information) or by LA-ICP-MS (single cell). Once the cultured cells were confluent, they were supplemented with different concentrations of nude AuNCs: 0, 5, 25 and 50 μg mL^{-1} in DMEMF12 (10% FBS 1% of P/S) for 24 h (37 °C in a 5% CO_2 incubator). Higher AuNCs concentrations (up to 350 μg mL^{-1}) were tested, although they were not employed for quantification.

On one hand, conventional nebulization ICP-MS was employed to determine the average mass of Au per cell in suspensions containing HRPEsv cells@AuNCs, which were collected from the seeding chambers after the AuNCs internalisation process and after washing the medium (3 times with PBS) to remove free AuNCs that may exist in solution and could interfere with the values of gold internalized by the cells. For the quantification of gold, an external calibration with Au (III) liquid standards, was performed by ICP-MS analysis (see experimental conditions in Table S1). The protocols followed with the cells (washing steps, counting with haemocytometer and mineralization) are detailed at **Supplementary Material**.

On the other hand, HRPEsv cells@AuNCs standards were

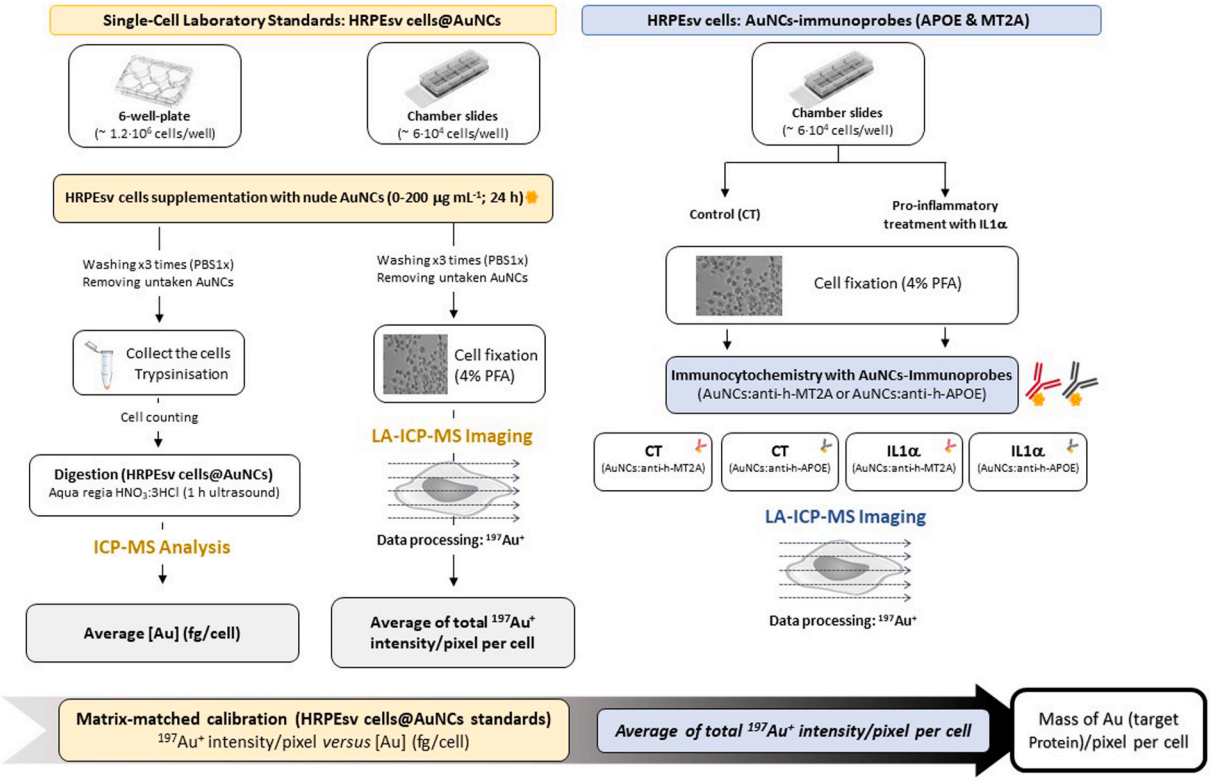

Fig. 1. Workflow of the proposed methodology.

individually analysed by LA-ICP-MS using the optimized experimental conditions shown in Table S1 (same imaging strategy than that used for the analysis of APOE and MT2A in HRPEsv cells). Fixed HRPEsv cells (cultured and treated in the chamber slides) were stored in the refrigerator with a small volume of PBS (200 μL) to avoid possible drying and cell breakage. Just before the measurement by LA-ICP-MS, the walls of the chamber slide were cautiously removed, and PBS was carefully drained. An average of 30 individual HRPEsv cells@AuNCs were analysed by LA-ICP-MS for each AuNCs concentration used for supplementation. In this case, a 2D-image of $^{197}Au^{+}$ signal for each individual cell was constructed using the Iolite (v4) software.

2.1.4. Imaging of APOE and MT2A proteins in individual HRPEsv cells by LA-ICP-MS

HRPEsv cells after being grown, subjected to IL1α (or CT) treatment, and fixed with 4% PFA in the chamber slides (as described in Section 2.1.1.) are subjected to the ICC assay using the immunoprobes for the sequential detection of APOE and MT2A. After the ICC assay, HRPEsv were analysed by LA-ICP-MS following the same protocol employed for the analysis of the "single-cell laboratory standards". In this case, $^{197}Au^{+}$ signal for each individual cell was related to the distribution of a specific protein along the cell. Depending on the AuNCs-immunoprobe employed (AuNCs:anti-h-APOE or AuNCs:anti-h-MT2), APOE or MT2A was detected, both in CT and IL1α−treated cells. As described above, a 2D-image of $^{197}Au^{+}$ signal for each individual cell was constructed using the Iolite (v4) software.

2.2. Instrumentation

Conventional nebulization ICP-MS analysis (7900 from Agilent) was employed for the determination of the average Au content in the cell suspensions to be used as single-cell laboratory standards. For LA-ICP-MS analysis, the excimer-based laser ablation system NWR193 (Elemental Scientific - ESI) equipped with a two-volume cell (TwoVol2 Ablation Cell, ESI) was coupled to the ICP-MS for the analysis of individual HRPEsv cells (both HRPEsv cells@AuNCs laboratory standards and HRPEsv cells submitted to the ICC assay with the AuNCs-immunoprobes were analysed by LA-ICP-MS) fixed onto the chamber slides. For the high-resolution analysis of specific areas, multiple line scanning mode with a spot size of 6 μm was applied. A laser pulse frequency of 20 Hz and a laser fluence of 0.3 J cm^{-2} ensured a quantitative ablation (Table S1 depicts the optimized experimental conditions). The $^{197}Au^{+}$ signal was acquired from AuNCs (HRPEsv cells@AuNCs standards) or AuNCs-immunoprobes (HRPEsv cells with the AuNCs-immunoprobe). Data processing (2D-images of $^{197}Au^{+}$ distribution in individual HRPEsv cells, histograms and selection of the cells regions) were performed with Iolite (v4) software. Thermal gradient was chosen as the scale for 2D images and expand by interpolating filter was applied for data treatment.

To study the proteins distribution in HRPEsv cells by fluorescence detection, a laser confocal microscope (DM IRE2; Leica) with a 63× oil immersion objective was employed. Images with both lateral (xy axis) and depth (yz or xz axis) resolution were obtained.

3. Results and discussion

3.1. Optimizations of the immunocytochemistry assay with AuNCs-immunoprobes

To develop a target protein quantification strategy in single cells using LA-ICP-MS and antibodies labelled with AuNCs, the characterization of the AuNCs-immunoprobes was performed to determine the amplification factor (i.e., the number of Au atoms labelled per available antibody). Following a strategy previously reported [21], 466 Au atoms on average (466 ± 18) was found as the amplification factor for AuNCs:anti-h-APOE and AuNCs:anti-h-MT2A immunoprobes (**Supplementary Material** collects a description of the procedure).

Optimization of the primary antibodies concentration in both immunoprobes was performed to ensure the total recognition of APOE and MT2A in HRPEsv cells. First, following the dilution range recommended for the antibodies specifications, three serial dilutions of the antibodies stock concentration were independently assayed in CT and IL1α−treated HRPEsv cells (1 mg mL^{-1} and 0.23 mg mL^{-1} were the anti-h-APOE and anti-h-MT2A stock concentrations, respectively). An ICC assay using secondary antibodies labelled with Alexa® fluorophore for fluorescent detection was employed for such purpose. Fluorescence measurement of Alexa®488 and Alexa®594 was performed for anti-h-APOE and anti-h-MT2A antibodies, respectively. As an example, Fig. S1 depicts the fluorescence images obtained for the APOE and MT2A distribution in CT HRPEsv cells. A 1:100 dilution (10 μg mL^{-1}) for anti-h-APOE (Fig. S1c) and 1:46 dilution (5 μg mL^{-1}) for anti-h-MT2A (Fig. S1g) were found as optimum for the complete detection of the target cytosolic proteins in HRPEsv cells. A deeper description of the studies related to the selection of antibodies concentration is collected at **Supplementary Material**.

3.2. Immunolocalization of cytosolic proteins in individual HRPEsv cells by LA-ICP-MS

The use of AuNCs as a single immunoprobe label for the sequential study of APOE and MT2A in HRPEsv cells allowed to determine the qualitative distribution of the two cytosolic proteins by fluorescence microscopy and LA-ICP-MS. Concerning LA-ICP-MS, 2D-images of $^{197}Au^{+}$ signal (i.e., APOE or MT2A distribution depending on the AuNCs-immunoprobe employed) were obtained for CT and IL1α−-treated HRPEsv cells. In the case of APOE, Fig. 2 collects the 2D-images obtained by LA-ICP-MS for $^{197}Au^{+}$ intensity using AuNCs:anti-h-APOE immunoprobe (i.e., APOE distribution) in CT (Fig. 2a) and IL1α−-treated HRPEsv cells (Fig. 2c). Additionally, Fig. 2b and **d** show the merge of the optical image of HRPEsv cells before LA sampling and the $^{197}Au^{+}$ signal to further understand the protein distribution along the cells structure. Intrinsic biological variability and expected cell-to-cell differences contributed to hinder predicting common behaviour in the whole cells population, although some tendencies were observed. APOE was localized throughout the cytoplasm, mainly present in the perinuclear region (e.g., cells #2 and #4 showed a higher level close to the nucleus) and showing almost absent within the nucleus (e.g., cells #1 and #5). Similar qualitative distribution of APOE was found regardless the cells treatment (i.e., CT or IL1α−treated).

In addition to qualitative 2D-images, histograms for each individual HRPEsv cell analysed by LA-ICP-MS were studied. Histograms allowed to get a better knowledge of the intracellular target cytosolic proteins distribution due to the biological variability or to the effect of pro-inflammatory treatment. They also helped overcome the required adjustment of the intensity scale when several cells were collected in the same image (i.e., scales were adjusted to avoid "burnt" intensity images, but some regions of the cells could be then undetectable in the images). Fig. S2 shows the histogram obtained for two CT and two IL1α−treated HRPEsv individual cells (2D-images of the cells are in Fig. 2), representing the number of pixels for each $^{197}Au^{+}$ intensity. As can be seen, (i) A large percentage of the cells area analysed by LA-ICP-MS (i.e., a high number of pixels) presented low $^{197}Au^{+}$ intensity signals, indicating low protein levels, and (ii) A high variability was observed for the maximum $^{197}Au^{+}$ intensity (ranging from 20,000 to 125,000 cps), which can be attributed to intrinsic biological variability of cultured cells, both in CT and IL1α−treated conditions.

Taking advantage of the bimodal detection that can be achieved with AuNCs-immunoprobes, APOE was also localized in HRPEsv cells by laser confocal microscopy (λ_{ex} = 400 nm; λ_{em} = 650–750 nm). Such measurements confirmed the antibody penetration through the whole cell structure (in-depth fluorescence measurements). Fig. 3a–d show the fluorescence images obtained for APOE distribution following AuNCs

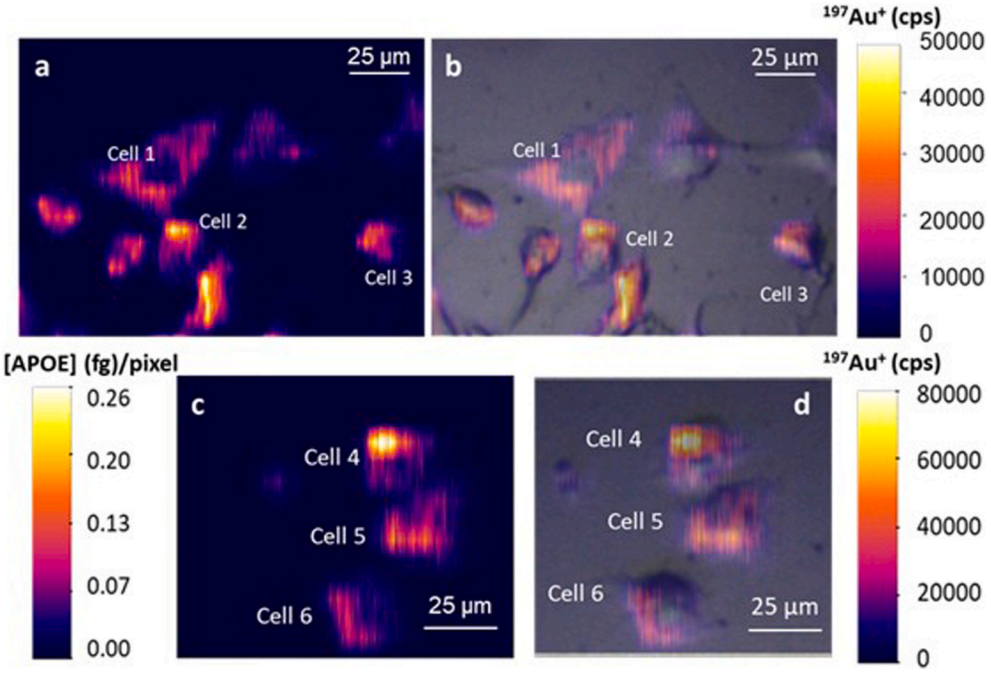

Fig. 2. Qualitative 2D-images obtained by LA-ICP-MS for $^{197}Au^{+}$ signal (cps) using AuNCs:anti-h-APOE immunoprobe in CT and IL1 α−treated HRPEsv cells. a) APOE distribution in CT cells, b) Merge of $^{197}Au^{+}$ signal and optical image of the CT cells before LA sampling, c) APOE distribution in IL1 α−treated cells, d) Merge of $^{197}Au^{+}$ signal and optical image of the IL1 α−treated cells before LA sampling. In addition to the colour scales following $^{197}Au^{+}$ intensity (cps) per pixel, the quantitative distribution of APOE in cell #4 is indicated in the left scale (expressed as the mass of APOE in fg per pixel). (For interpretation of the references to colour in this figure legend, the reader is referred to the Web version of this article.)

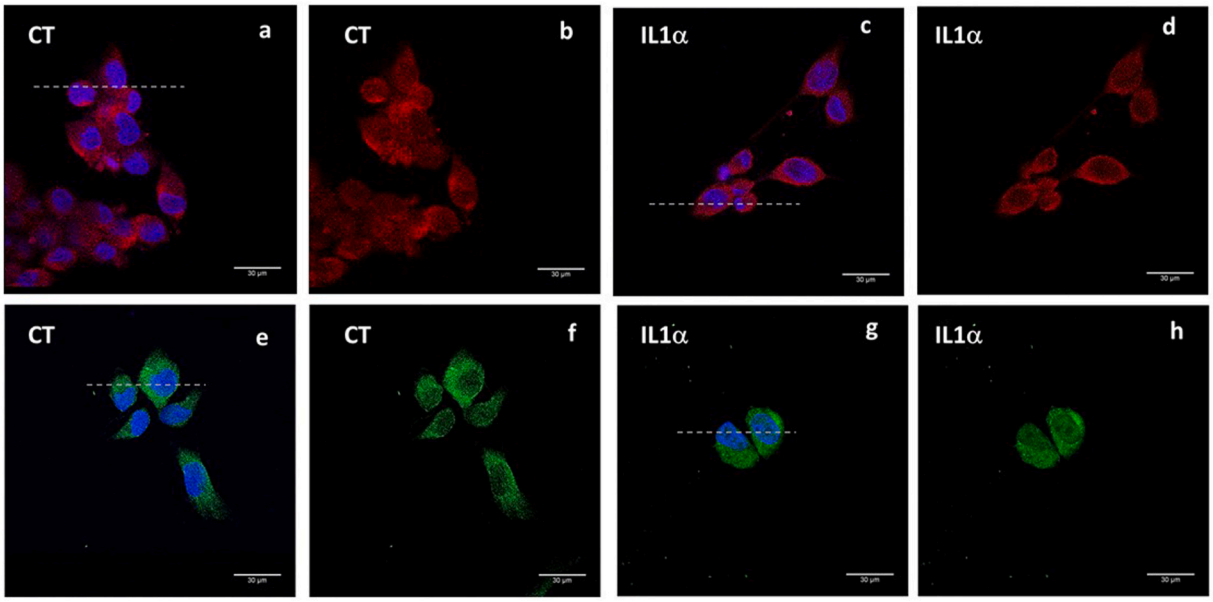

Fig. 3. Fluorescence images obtained by laser confocal microscopy for APOE distribution in CT and IL1 α−treated HRPEsv cells. a & b) CT cells; DAPI (blue) and AuNCs:anti-h-APOE immunoprobe (APOE distribution in red), c & d) IL1 α−treated cells; DAPI and AuNCs:anti-h-APOE immunoprobe, e & f) CT cells; DAPI (blue) and secondary antibody Fluor Alexa®488 (APOE distribution in green), g & h) IL1 α−treated cells; DAPI and secondary antibody Fluor Alexa®488. Note that dotted lines (a, c, e and f) mark the position for the in-depth images of Fig. S3. (For interpretation of the references to colour in this figure legend, the reader is referred to the Web version of this article.)

emission for CT and IL1α−treated HRPEsv cells and Fig. 3e–h collect the fluorescence images obtained by the indirect fluoroimmunoassay using Alexa® 488 (for validation purposes). As can be observed, APOE distribution found in HRPEsv cells by LA-ICP-MS for CT and IL1α−treated cells was in agreement with fluorescence images, both using direct and indirect detection. In addition, in-depth fluorescence measurements (z-axis) using Alexa® fluorophore confirmed the lower presence of APOE protein within the cell nuclei compared to the high perinuclear and cytoplasmic intensity observed (see Fig. S3). The total penetration of AuNCs-immunoprobe (i.e., anti-h-APOE antibody) inside the cells was also confirmed by observing fluorescence emission within the whole cell volume. Note that negative controls were always evaluated to ensure nonspecific interactions coming from the primary antibody or the AuNCs (Fig. S4 shows the fluorescence image obtained for AuNCs negative controls in CT and IL1α−treated cells, demonstrating the absence of unspecific interactions).

Concerning MT2A, an APOE-like protocol was followed using AuNCs:anti-h-MT2A immunoprobe. Fig. 4 shows the 2D-images obtained by LA-ICP-MS for $^{197}Au^{+}$ intensity in CT (Fig. 4a) and IL1α−-treated HRPEsv cells (Fig. 4c); Fig. 4b and **d** show the merge of the

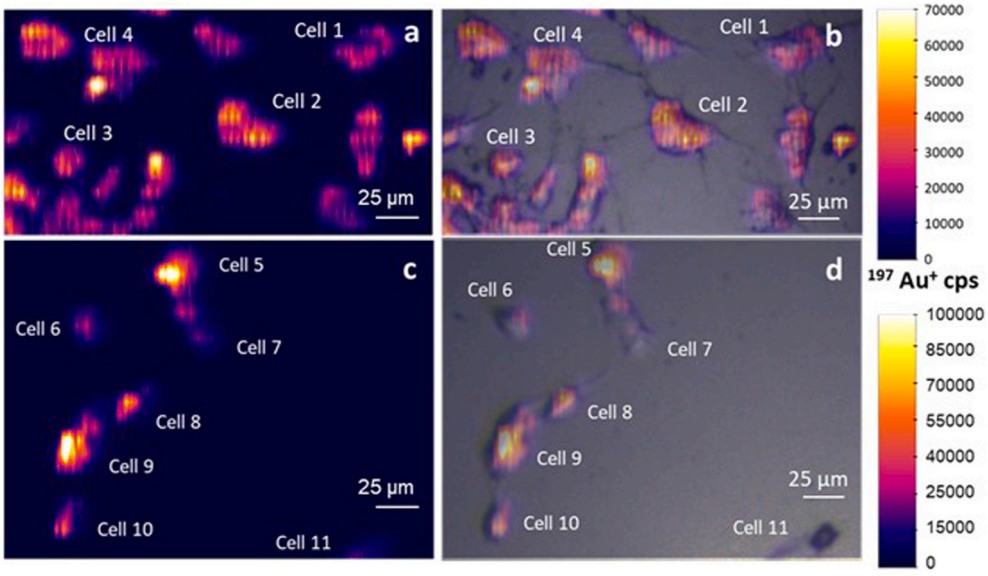

Fig. 4. Qualitative 2D-images obtained by LA-ICP-MS for $^{197}Au^{+}$ signal (cps) using AuNCs:anti-h-MT2A immunoprobe in CT and IL1 α−treated HRPEsv cells. a) MT2A distribution in CT cells, b) Overlapping of $^{197}Au^{+}$ signal and optical image of the CT cells before LA sampling, c) MT2A distribution in IL1 α−treated cells, b) Overlapping of $^{197}Au^{+}$ signal and optical image of the IL1 α−treated cells before LA sampling.

optical images and the $^{197}Au^{+}$ signal. In contrast to APOE, MT2A was homogeneously distributed within the cytoplasm with a higher presence at nucleus (e.g., cells #2 and #3 in CT and cells #5 and #9 in IL1α). Variability of intracellular accumulation of MT2A was high but it agreed with the protein distribution found by fluorescence microscopy (Fig. S1). Additionally, the homogeneous distribution observed for MT2A along the cell as well as the absence of significant changes between CT and IL1α regarding its localization is consistent with previous studies [22]. Histograms were also studied for MT2A in CT and IL1α−treated cells (Fig. S5). In this case, MT2A was more homogeneously localized within the whole cell, since a large number of pixels exhibited $^{197}Au^{+}$ signals in the order of 10,000–40,000 cps. For IL1α−treated cells, a large percentage of the cells area presented low $^{197}Au^{+}$ signals (indicating low protein levels), whereas there were also specific regions of the cells were $^{197}Au^{+}$ signals showed higher signals (up to 125,000 cps), suggesting an accumulation of MT2A (probably attributed to the nucleus region identified in Fig. 4).

3.3. *HRPEsv cells supplemented with AuNCs as laboratory standards for matrix-matched calibration by LA-ICP-MS*

In the present study, the quantitative imaging of APOE and MT2 in CT and IL1α−treated HRPEsv cells was pursued. For such purpose, external calibration based on the use of HRPEsv cells supplemented with nude AuNCs as single-cell laboratory standards was proposed. As described in the experimental section and is summarised in Fig. 1, cells were incubated with different concentrations of nude AuNCs and these HRPEsv cells@AuNCs standards were subsequently characterised by conventional nebulization ICP-MS and LA-ICP-MS.

On one hand, conventional nebulization ICP-MS analysis was used to determine the average mass of Au in the cells population for the different AuNCs concentrations added for supplementation. In such way, the Au concentration in HRPEsv cells@AuNCs standards was measured (after counting the cells and its mineralization) using external calibration with Au (III) standard solutions. Different AuNCs concentrations were studied for cells supplementation (up to 350 µg mL^{-1}). However, cell viability decreased dramatically after incubation of the cells at high AuNCs concentration (24 h treatment) [23] and 50 µg mL^{-1} was the maximum amount used for HRPEsv cells@AuNCs standards. As can be seen in Fig. S6, a linear behaviour was observed for the average concentration of Au found in HRPEsv cells@AuNCs standards (expressed as fg of Au per cell) compared to the AuNCs concentration used for supplementation. Note that it was observed a limit for the AuNCs uptake from the cells; the use of AuNCs concentrations higher than 50 µg mL^{-1} gave rise to a plateau in the mass of Au detected in the cells.

On the other hand, HRPEsv cells@AuNCs calibration standards prepared in chamber slides and supplemented with different concentrations of AuNCs concentrations (0, 5, 25, 50, 100 and 200 µg mL^{-1}) were individually analysed by LA-ICP-MS. In this case, the imaging of the intracellular AuNCs uptake was carried out by LA-ICP-MS measuring 30 cells per condition. For each single cell analysed by LA-ICP-MS, a specific data treatment strategy was developed. As an example, Fig. 5 collects some images for three individual cells from the supplementation with 5 µg mL^{-1} AuNCs. Data processing of HRPEsv cells@AuNCs standards were always performed as follows using Iolite (v4) software: i) A 2-D image of $^{197}Au^{+}$ distribution (in cps) was obtained for individual HRPEsv cells by LA-ICP-MS analysis (Fig. 5a); ii) An optical image of each cell (taken just before LA sampling) was used for comparison with the $^{197}Au^{+}$ image (Fig. 5b); ii) The area of each individual cell were specifically marked in the 2-D qualitative image of $^{197}Au^{+}$ (red surface in Fig. 5c), following the cell surface from the optical image. Thus, it was possible to obtain a value of the area of each cell expressed in pixels. In this particular example, 717, 815 and 889 pixels were found for cells #1, #2 and #3, respectively. Note that the area of the cell cannot be directly selected from the $^{197}Au^{+}$ image since there was not a homogeneous distribution of AuNCs in the whole cells surface. iii) The total $^{197}Au^{+}$ intensity for each cell were calculated as the sum of $^{197}Au^{+}$ intensities from the pixels that compose the cell ($1.10{\cdot}10^{6}$ cps, $9.78{\cdot}10^{5}$ cps and $8.77{\cdot}10^{5}$ cps for cells #1, #2 and #3, respectively); and iv) $^{197}Au^{+}$ intensity was normalized by the cells size (i.e., the number of pixels which define each cell). In the example collected in Fig. 5 and $1.53{\cdot}10^{3}$ cps, $1.14{\cdot}10^{3}$ cps and $9.86{\cdot}10^{2}$ cps were found as the average $^{197}Au^{+}$ intensity per pixel. HRPEsv cells@AuNCs standards for the different AuNCs supplementation treatments were analysed by LA-ICP-MS and processed following the proposed strategy. Fig. S7 collects the 2D-images obtained for single-cell laboratory standards using 25 µg mL^{-1} and 50 µg mL^{-1} AuNCs concentration for supplementation.

After the analysis by conventional nebulization ICP-MS and LA-ICP-MS of the single-cell laboratory standards for each AuNCs supplementation condition, and the corresponding data treatment, a calibration

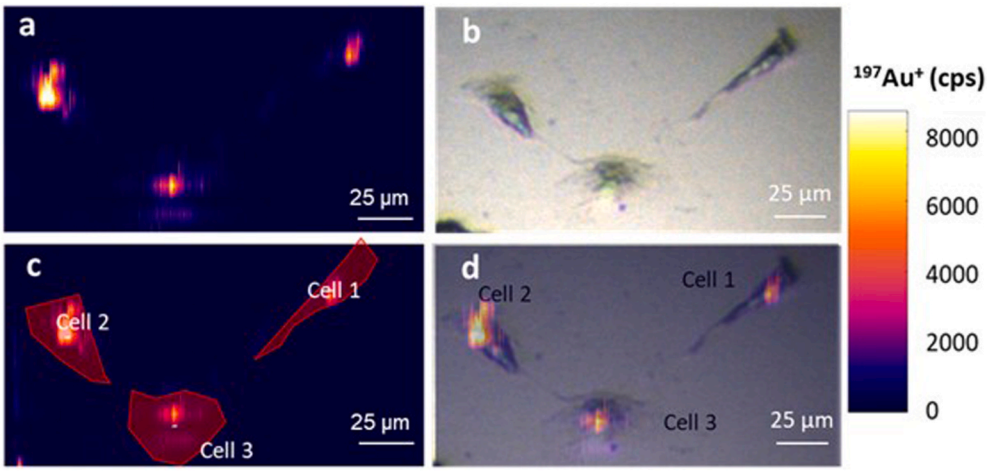

Fig. 5. Analysis of HRPEsv cells@AuNCs standards (supplementation of HRPEsv cells with 50 mg mL^{-1} AuNCs, 24 h) by LA-ICP-MS. a) Qualitative 2D-image representing $^{197}Au^{+}$ intensity (cps), b) Optical image of the cells before LA sampling, c) Definition of the area corresponding to each individual marked in red, and d) Overlapping of $^{197}Au^{+}$ signal and optical image of the cells before LA sampling. (For interpretation of the references to colour in this figure legend, the reader is referred to the Web version of this article.)

graph was constructed representing the average $^{197}Au^{+}$ intensity per pixel for each cell (determined by LA-ICP-MS analysis) *versus* the Au concentration of the HRPEsv cell@AuNCs standards (determined by conventional nebulization ICP-MS). Fig. S8 shows the Au calibration graph obtained that was further used for the determination of APOE and MT2A concentration in CT and IL1α−treated HRPEsv cells. At this point it should be highlighted that both the intrinsic biological variability within the HRPEsv cells culture and the possible differences in the AuNCs uptake contributed to the uncertainty of the measurements, as expected. Fig. 6 depicts the box plot for the average $^{197}Au^{+}$ intensity per cell obtained by LA-ICP-MS for different AuNCs supplementation treatments (in this case 0–200 μg mL^{-1} AuNCs concentration were represented). Note that uptake of AuNCs increased in a dose-dependent manner up to the cellular saturation observed by the plateau at 50 μg mL^{-1} and above AuNCs concentrations (upper value employed for quantification purposes). Relative standard deviation values ranged from 9% to 22% (analysis of 30 individual cells per condition).

3.4. Determination of APOE and MT2A concentrations in HRPEsv cells by LA-ICP-MS using single-cell laboratory standards

The proposed quantitative imaging methodology based on the use of HRPEsv cells@AuNCs standards was applied to sequentially study the APOE and MT2A content in CT and IL1α−treated cells by LA-ICP-MS. Using the obtained linear regression with the HRPEsv cells@AuNCs standards (Fig. S8) and calculating the total intensity of $^{197}Au^{+}$ per cell in CT and IL1α −treated HRPEsv cells (following the procedure described for the single-cell laboratory standards), the total mass of Au per cell was determined (at a first step expressed as fg of Au per cell). Next, the total mass of Au per cell was converted into the target protein mass per cell (APOE or MT2A depending on the AuNCs-immunoprobe used) following a protocol previously reported for tissue sections [21, 24].

The APOE mass obtained by LA-ICP-MS for each individual cell of both CT and IL1α−treated HRPEsv cells are collected in Table 1. The Table summarizes the individual values obtained for 22 CT and 11 IL1α−treated cells analysed with the proposed methodology. It can be seen that the average APOE mass for each condition indicated a decrease on the protein levels from 27.2 ± 7.9 fg of APOE/cell for CT cells to 16.0 ± 5.8 fg of APOE/cell for IL1α−treated cells (0.58-fold change). Such lessen in the protein levels of HRPEsv cells subjected to the pro-inflammatory treatment with IL1α was confirmed by qPCR at RNA expression level, where a decreasing about 30% of the gene expression was observed (Fig. S9). Additionally, the mass of APOE determined by

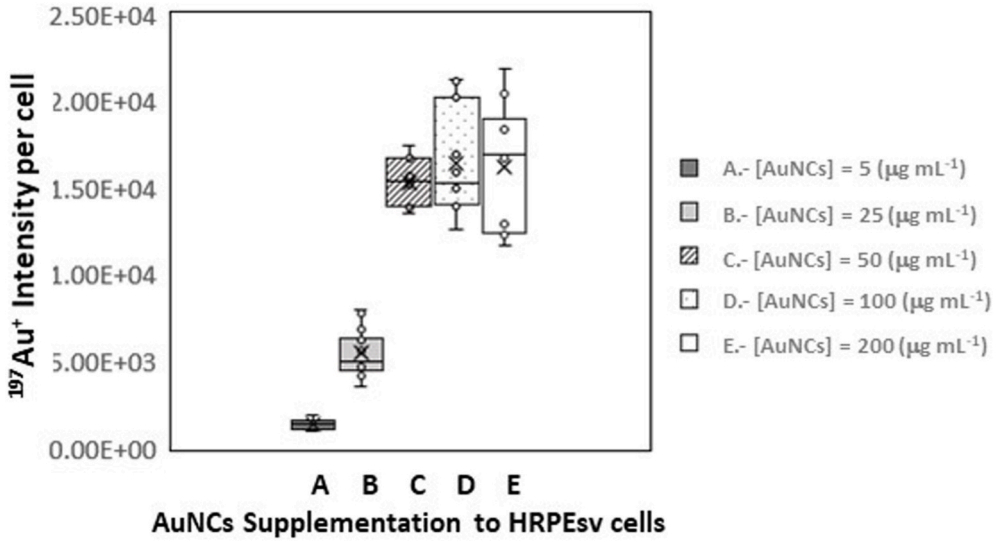

Fig. 6. Box and whisker plot representing the average $^{197}Au^{+}$ intensity per cell (determined by LA-ICP-MS analysis) for the different HRPEsv cells@AuNCs standards obtained through the supplementation of HRPEsv cells with different AuNCs concentrations (0–200 mg mL^{-1}). Error bars correspond to the standard deviation calculated for the analysis of 30 individual cells per condition.

Table 1
Experimental results obtained for the mass of APOE per cell in CT and IL1α−treated HRPEsv cells analysed by LA-ICP-MS using AuNCs-immunoprobe as the elemental label and HRPEsv cells@AuNCs standards for calibration.

	Cell	Total Intensity (cps)	Cell size (pixels)	$^{197}Au^{+}$ (Int./pixel)	Au mass (fg/cell)	APOE mass (fg/cell)	APOE mass (fg/cell)
APOE - CT	1	8.19E+06	594	1.38E+04	80.20	29.7	**27.2 ± 7.9**
	2	6.56E+06	770	8.52E+03	49.53	18.3	
	3	7.22E+06	543	1.33E+04	77.34	28.6	
	4	1.07E+07	1031	1.04E+04	60.53	22.4	
	5	7.45E+06	587	1.27E+04	73.79	27.3	
	6	1.22E+07	803	1.52E+04	88.51	32.8	
	7	5.64E+06	512	1.10E+04	63.99	23.7	
	8	1.17E+07	606	1.93E+04	112.39	41.6	
	9	7.82E+06	494	1.58E+04	92.04	34.1	
	10	1.04E+07	666	1.56E+04	90.69	33.6	
	11	8.09E+06	640	1.26E+04	73.47	27.2	
	12	1.08E+07	1149	9.38E+03	54.54	20.2	
	13	3.83E+06	424	9.04E+03	52.57	19.5	
	14	3.53E+06	415	8.50E+03	49.42	18.3	
	15	1.34E+07	1732	7.71E+03	44.82	16.6	
	16	6.84E+06	817	8.37E+03	48.66	18.0	
	17	9.05E+06	882	1.03E+04	59.67	22.1	
	18	1.42E+07	1108	1.28E+04	74.32	27.5	
	19	5.52E+06	456	1.21E+04	70.42	26.1	
	20	1.00E+07	542	1.85E+04	107.26	39.7	
	21	2.31E+07	1132	2.04E+04	118.42	43.8	
	22	1.72E+07	1294	1.33E+04	77.12	28.5	
APOE – IL1α	1	5.30E+06	634	8.36E+03	48.63	18.0	**16.0 ± 5.8**
	2	5.30E+06	634	8.36E+03	48.63	18.0	
	3	6.07E+06	655	9.27E+03	53.87	19.9	
	4	4.06E+06	726	5.59E+03	32.51	12.0	
	5	7.24E+06	658	1.10E+04	63.96	23.7	
	6	5.09E+06	1104	4.61E+03	26.80	9.9	
	7	6.90E+06	639	1.08E+04	62.77	23.2	
	8	4.83E+06	1460	3.31E+03	19.24	7.1	
	9	5.35E+06	789	6.79E+03	39.45	14.6	
	10	3.53E+06	840	4.21E+03	24.45	9.0	
	11	5.51E+06	568	9.70E+03	56.40	20.9	

LA-ICP-MS using AuNCs-immunoprobe was validated by the determination of APOE concentration using a quantitative ELISA kit. The APOE mass determined by the ELISA was found to be 17.94 ± 1.30 fg APOE/cell for CT cells and 10.19 ± 0.53 fg APOE/cell for IL1α−treated cells (0.56-fold change). These results were in agreement with the protein content determined by LA-ICP-MS, confirming a lower expression of APOE after the pro-inflammatory stress. Similar results were also reported in a recent study carried out by sc-ICP-MS [25]. It should be highlighted that using the proposed methodology by LA-ICP-MS not only the total mass of protein per cell but also the quantitative distribution of the target protein can be studied. As an example, the APOE distribution expressed as fg of protein per pixel is shown in Fig. 2 (panel c) for cell #4.

MT isoforms play an important role during inflammatory processes and oxidative stress conditions, being widely studied on eye diseases related to oxidative processes [26]. Table S2 shows the mass obtained for MT2A by LA-ICP-MS for CT and IL1α−treated HRPEsv cells (individual values for 23 CT and 14 IL1α−treated cells are collected). As can be observed in the averaged results, the treatment of HRPEsv cells with 100 ng mL^{-1} of IL1α during 48 h produced an upregulation of MT2A synthesis in the cells, from 2.1 ± 0.9 fg/cell of MT2A in CT to 4.6 ± 1.6 fg/cell of MT2A in IL1α−treated cells (2.1-fold change). qPCR analysis confirmed this increase at the gene expression level for MT2A (Fig. S9) and the protein mass obtained using a quantitative ELISA kit was also in agreement with the experimental results obtained by LA-ICP-MS. The MT2A mass determined by the quantitative ELISA kit was 1.74 ± 0.28 fg MT2A/cell for CT and 3.36 ± 0.50 fg MT2A/cell for IL1α-treated HRPEsv cells (1.9-fold change), confirming an overexpression of MT2A after the treatment with IL1α. The same tendency for MT2A (i.e., an overexpression of the protein after the pro-inflammatory treatment) in HRPEsv cells was observed by sc-ICP-MS using AuNCs-immunoprobe [25].

4. Conclusions

In this work, a matrix-matched calibration strategy was successfully developed for the first time with the aim of overcoming the current limitations regarding LA-ICP-MS quantification in cultured cells. In order to fully mimic the complex cell matrix, HRPEsv cells were supplemented with increasing concentrations of suspensions containing nude AuNCs to generate single-cell laboratory standards (HRPEsv cells@AuNCs). A complete characterization of HRPEsv cells@AuNCs standards were carried out by conventional nebulization ICP-MS and LA-ICP-MS, and a data treatment strategy was developed for each single cell analysed by LA-ICP-MS. This strategy allowed the quantitative imaging of protein expression on a cell-to-cell basis, which is really interesting due to the heterogeneity of the cell populations. It should be noted that smaller laser beam sizes than 6 μm could be carried out in further studies to obtain images of the protein distribution throughout individual cells with a better lateral resolution.

As a proof of concept, the sequential determination of MT2A and APOE in individual HRPEsv cells was carried out by LA-ICP-MS in cells subjected to inflammation with the cytokine Interleukin-1α and controls. A single biomarker strategy using immunoprobes labelled with fluorescent monodisperse AuNCs (1.90 ± 0.4 nm) was performed to study the distribution of APOE and MT2A in single cells (about 30 μm diameter size) with a subcellular resolution. The average results of MT2A and APOE amounts obtained with the proposed methodology were in agreement with the quantitative results obtained by commercial ELISA kits, indicating that APOE levels diminished after the pro-inflammatory treatment whereas MT2A showed an overexpression of the protein after the treatment. It should be stressed that using the proposed methodology by LA-ICP-MS not only the total mass of protein per cell (that will be possible to achieved by sc-ICP-MS) but also the quantitative distribution of the target protein can be determined.

The average mass of APOE and MT2A per cell found with the proposed strategy is in agreement with the results previously obtain by single cell (sc)-ICP-MS. It should be noted that sc-ICP-MS provides a very fast means for cell-to-cell analysis and, therefore, results could be as representative of the cell culture heterogeneities since thousands of cells can be measured in just a few seconds. However, LA-ICP-MS is well-stablished as a complementary technique since the cell analysis throughput is much lower, but it allows to obtain the proteins distribution within the cell.

Note that our work opens the way to further studies in cell cultures using LA-ICP-MS and other metal NCs (e. g., Pt, Ir, Pd) to understand the role of biomolecules at cellular level in biological processes. Additionally, the simultaneous determination of different proteins in single cells will be accessible by using different metal NCs together with a time-of-flight mass spectrometer.

CRediT authorship contribution statement

Ana Lores-Padín: Investigation, Methodology, Writing – original draft. **Beatriz Fernández:** Conceptualization, Supervision, Writing – review & editing. **Montserrat García:** Resources, Visualization. **Héctor González-Iglesias:** Visualization, Conceptualization. **Rosario Pereiro:** Supervision, Funding acquisition, Writing – review & editing.

Declaration of competing interest

The authors declare that they have no known competing financial interests or personal relationships that could have appeared to influence the work reported in this paper.

Acknowledgements

This work was financially supported through project PID2019-107838RB-I00/Agencia Estatal de Investigación (AEI)/10.13039/501100011033). A. Lores-Padín acknowledges the FPU Grant (Ref. MECD-17-FPU16/01363; Ministry of Education). Authors would like to acknowledge the technical support provided by Servicios Científico-Técnicos of the University of Oviedo.

Appendix A. Supplementary data

Supplementary data to this article can be found online at https://doi.org/10.1016/j.aca.2022.340128.

References

[1] F. Calderón-Celis, J. Ruiz-Encinar, A reflection on the role of ICP-MS in proteomics: update and future perspective, J. Proteonomics 198 (2019) 11–17. https://doi:10.1016/j.jprot.2018.11.010.

[2] P.E. Oomen, M.A. Aref, I. Kaya, N.T.N. Phan, A.G. Ewing, Chemical analysis of single cells, Anal. Chem. 91 (2019) 588–621, https://doi.org/10.1021/acs.analchem.8b04732.

[3] M. Corte-Rodríguez, R. Alvarez-Fernandez, P. García-Cancela, M. Montes-Bayon, J. Bettmer, Single cell ICP-MS using online sample introduction systems: current developments and remaining challenges, Trends Anal. Chem. 132 (2020), 116042, https://doi.org/10.1016/j.trac.2020.116042.

[4] D. Pozebon, G.L. Scheffler, V.L. Dressler, Recent applications of laser ablation inductively coupled plasma mass spectrometry (LA-ICP-MS) for biological sample analysis: a follow-up review, J. Anal. At. Spectrom. 32 (2017) 890–919, https://doi.org/10.1039/C7JA00026J.

[5] P.A. Doble, R. Gonzalez-de-Vega, D.P. Bishop, D.J. Hare, D. Clases, Laser ablation-inductively coupled plasma-mass spectrometry imaging in biology, Chem. Rev. 121 (2021) 11769–11822, https://doi.org/10.1021/acs.chemrev.0c01219.

[6] M. Cruz-Alonso, A. Lores-Padín, E. Valencia, H. González-Iglesias, B. Fernández, R. Pereiro, Quantitative mapping of specific proteins in biological tissues by laser ablation–ICP-MS using exogenous labels: aspects to be considered, Anal. Bioanal. Chem. 411 (2019) 549–558, https://doi.org/10.1007/s00216-018-1411-1.

[7] T. Büchner, D. Drescher, V. Merk, H. Traub, P. Guttmann, S. Werner, N. Jakubowski, G. Schneiderd, J. Kneipp, Biomolecular environment, quantification, and intracellular interaction of multifunctional magnetic SERS nanoprobes, Analyst 141 (2016) 5096–5106, https://doi.org/10.1039/C6AN00890A.

[8] S. Rodríguez-Menéndez, B. Fernández, H. González-Iglesias, M. García, L. Álvarez, J.I. García-Alonso, R. Pereiro, Isotopically enriched tracers and inductively coupled plasma mass spectrometry methodologies to study zinc supplementation in single-cells of retinal pigment epithelium in vitro, Anal. Chem. 91 (2019) 4488–4495, https://doi.org/10.1021/acs.analchem.8b05256.

[9] S. Yamashita, Y. Yoshikuni, H. Obayashi, T. Suzuki, D. Green, T. Hirata, Simultaneous determination of size and position of silver and gold nanoparticles in onion cells using laser ablation-ICP-MS, Anal. Chem. 91 (2019) 4544–4551. https://10.1021/acs.analchem.8b05632.

[10] D. Drescher, C. Giesen, H. Traub, U. Panne, J. Kneipp, N. Jakubowski, Quantitative imaging of gold and silver nanoparticles in single eukaryotic cells by laser ablation ICP-MS, Anal. Chem. 84 (2012) 9684–9688, https://doi.org/10.1021/ac302639c.

[11] M.G. Mello, M.T. Westerhausen, P. Singh, P.A. Doble, J. Wanagat, D.P. Bishop, Assessing the reproducibility of labelled antibody binding in quantitative multiplexed immuno-mass spectrometry imaging, Anal. Bioanal. Chem. 413 (2021) 5509–5516. https://10.1007/s00216-021-03536-9.

[12] C. Giesen, H.A.O. Wang, D. Schapiro, N. Zivanovic, A. Jacobs, B. Hattendorf, P. J. Schüffler, D. Grolimund, J.M. Buhmann, S. Brandt, Z. Varga, P.J. Wild, D. Günther B. Bodenmiller, Highly multiplexed imaging of tumor tissues with subcellular resolution by mass cytometry, Nat. Methods 11 (2014) 417–422. https://10.1038/nmeth.2869.

[13] A. Arakawa, N. Jakubowski, S. Flemig, G. Koellensperger, M. Rusz, D. Iwahata, H. Traub, T. Hirata, High-resolution laser ablation inductively coupled plasma mass spectrometry used to study transport of metallic nanoparticles through collagen-rich microstructures in fibroblast multicellular spheroids, Anal. Bioanal. Chem. 411 (2019) 3497–3506. https://10.1007/s00216-019-01827-w.

[14] A. Arakawa, N. Jakubowski, G. Koellensperger, S. Theiner, A. Schweikert, S. Flemig, D. Iwahata, H. Traub, T. Hirata, Quantitative imaging of silver nanoparticles and essential elements in thin sections of fibroblast multicellular spheroids by high resolution laser ablation inductively coupled plasma time-of-flight mass spectrometry, Anal. Chem. 91 (2019) 10197–10203, https://doi.org/10.1021/acs.analchem.9b02239.

[15] M. Wang, L.N. Zheng, B. Wang, H.Q. Chen, Y.L. Zhao, Z.F. Chai, H.J. Reid, B. L. Sharp, W.Y. Feng, Quantitative analysis of gold nanoparticles in single cells by laser ablation inductively coupled plasma-mass spectrometry, Anal. Chem. 86 (2014) 10252–10256, https://doi.org/10.1021/ac502438n.

[16] S.J.M. van Malderen, E. Vergucht, M. De Rijcke, C. Janssen, L. Vincze, F. Vanhaecke, Quantitative determination and subcellular imaging of Cu in single cells via laser ablation-ICP-mass spectrometry using high-density microarray gelatin standards, Anal. Chem. 88 (2016) 5783–5789, https://doi.org/10.1021/acs.analchem.6b00334.

[17] T. Van Acker, T. Buckle, S.J.M. Van Malderen, D.M. Van Willigen, V. Van Unen, F. W.B. Van Leeuwen, F. Vanhaecke, High-resolution imaging and single-cell analysis via laser ablation-inductively coupled plasma-mass spectrometry for the determination of membranous receptor expression levels in breast cancer cell lines using receptor-specific hybrid tracers, Anal. Chim. Acta 1074 (2019) 43–53. https://10.1016/j.aca.2019.04.064.

[18] J. Zhai, Y. Wang, C. Xu, L. Zheng, M. Wang, W. Feng, L. Gao, L. Zhao, R. Liu, F. Gao, Y. Zhao, Z. Chai, X. Gao, Facile approach to observe and quantify the αIIbβ3 integrin on a single-cell, Anal. Chem. 87 (2015) 2546–2549, https://doi.org/10.1021/ac504639u.

[19] J. Zhai, L. Zhao, L. Zheng, F. Gao, L. Gao, R. Liu, Y. Wang, X. Gao, Peptide−Au cluster probe: precisely detecting epidermal growth factor receptor of three tumor cell lines at a single-cell level, ACS Omega 2 (2017) 276–282. https://10.1021/acsomega.6b00390.

[20] X. Zhang, R. Liu, Q. Shu, Q. Yuan, G. Xing, X. Gao, Quantitative analysis of multiple proteins of different invasive tumor cell lines at the same single-cell level, Small 14 (2018), 1703684. https://10.1002/smll.201703684.

[21] M. Cruz-Alonso, B. Fernández, M. García, H. González-Iglesias, R. Pereiro, Quantitative imaging of specific proteins in the human retina by LA-ICP-MS using bioconjugated metal nanoclusters as labels, Anal. Chem. 90 (2018) 12145–12151. https://10.1021/acs.analchem.8b03124.

[22] S. Rodríguez-Menéndez, M. García, B. Fernández, L. Álvarez, A. Fernández-Vega-Cueto, M. Coca-Prados, R. Pereiro, H. González-Iglesias, The zinc-metallothionein redox system reduces oxidative stress in retinal pigment epithelial cells, Nutrients 10 (2018) 1874, https://doi.org/10.3390/nu10121874.

[23] X. Cai, H.H. Chen, C.L. Wang, S.T. Chen, S.F. Lai, C.C. Chien, Y.Y. Chen, I. M. Kempson, Y. Hwu, C.S. Yang, G. Margaritondo, Imaging the cellular uptake of tiopronin-modified gold nanoparticles, Anal. Bioanal. Chem. 401 (2011) 809–816. https://10.1007/s00216-011-4986-3.

[24] A. Lores-Padín, B. Fernández, L. Álvarez, H. González-Iglesias, I. Lengyel, R. Pereiro, Multiplex bioimaging of proteins-related to neurodegenerative diseases in eye sections by laser ablation - inductively coupled plasma - mass spectrometry using metal nanoclusters as labels, Talanta 221 (2021), 121489. https://10.1016/j.talanta.2020.121489.

[25] A. Lores-Padín, E. Mavrakis, B. Fernandez, M. García, H. Gonzalez-Iglesias, R. Pereiro, S.A. Pergantis, Gold nanoclusters as elemental label for the sequential quantification of apolipoprotein E and metallothionein 2A in individual human cells of the retinal pigment epithelium using single cell-ICP-MS, Anal. Chim. Acta 1203 (2022), 33970, https://doi.org/10.1016/j.aca.2022.339701.

[26] A. Álvarez-Barrios, L. Álvarez, M. García, E. Artime, R. Pereiro, H. González-Iglesias, Antioxidant defenses in the human eye: a focus on metallothioneins, Antioxidants 11 (2021) 11–89, https://doi.org/10.3390/antiox10010089.